IL NUOVO CIMENTO Vol. 28 C, N. 4-5 Luglio-Ottobre 2005
DOI 10.1393/ncc/i2005-10095-3

Systematic analysis of X-ray GRB afterglows observed with XMM-Newton and Chandra(*)

B. Gendre(1), L. Piro(1) and M. DePasquale(2)
(1) *IASF - via Fosso del Cavaliere 100, 00133 Rome, Italy*
(2) *MSSL, Holmbury St. Mary - Dorking, Surrey RH5 6NT, UK*

(ricevuto il 23 Maggio 2005; pubblicato online il 19 Settembre 2005)

Summary. — We present a sample of GRB afterglows observed in the X-ray band with XMM-Newton or Chandra, focusing on the brightest events. We have derived for this sample the temporal slope and the spectral index of the continuum, and used closure relationships to discriminate the afterglow environment for each burst. We show that jet features are excluded most of the time, while ISM and wind environments cannot be discriminated. We finally focus on GRB040106, whose environment can be constrained by the X-ray observations only. For this burst, we present a broad-band analysis and derive some constraints on the positions of characteristic frequencies.

PACS 95.85.Nv – X-ray.
PACS 98.70.Rz – γ-rays sources; γ-ray bursts.
PACS 01.30.Cc – Conference proceedings.

1. – Introduction

While there is a growing sample of data for several tens of Gamma-Ray Bursts (GRBs), we still know very little about their environment and progenitor. According to the standard model, GRBs are produced by a blast wave which propagates into the medium surrounding an unspecified progenitor [9, 5, 6]. The nature of this surrounding medium depends on the progenitor nature, and is supposed to be either an InterStellar Medium of constant density (ISM) or a wind profile arising from a massive star which decreases in density with the distance to the star (hereafter wind model [2]). Features such as ultrarelativistic jets can complicate this model due to the symmetry change it can induce [10].

We have initiated a systematic analysis of all GRB X-ray afterglows observed so far in order to constrain the surrounding environment of GRBs. This can allow us to put constraints on the nature of the GRB progenitors. After the reduction and analysis of the Beppo-SAX observations [8], we present here the results we obtained with the XMM-Newton and Chandra observations.

(*) Paper presented at the "4th Workshop on Gamma-Ray Burst in the Afterglow Era", Rome, October 18-22, 2004.

2. – Sample used and data reduction

We retrieved all public data available from the archives of XMM-Newton and Chandra observation. The complete list of retrieved observations can be found in [4]. These observations were calibrated using the most up-to-date softwares. For the XMM-Newton EPIC (PN and MOS) data, we used the SAS version 6.0. For the Chandra data, we used CIAO version 3.1 and the calibration database CALDB version 2.27. The events were filtered using all provided GTI and standard filtering criteria (see [4]).

These filtered event files were checked for flaring background activities. We removed any period of such activity using a very strict condition (this can explain our discrepancies with other published works). We extracted spectra and light curves using circle regions; their radius are chosen to optimize the signal to noise ratio and take into account any possible neighbor source. The spectral and temporal backgrounds were extracted using a larger circular area free of sources at the same off-axis angle. We used for the spectral analysis XSPEC version 11.3.1 and for the temporal analysis the FTOOLS version 5.3 and a customized IDL script.

3. – Discussion and conclusions

3˙1. *Closure relationship and surrounding medium.* – The spectral index and the temporal decay of a burst are linked together [11, 2]. This relationship depends on the burst environment (wind or ISM), on jet features and on the cooling frequency position. This gives a set of six closure relationships which could give insights about the burst environment and/or jet features. We show in fig. 1 the calculation result of the six closure relationships for the best constrained bursts from our sample.

We can first note that Chandra observations are not very constraining. This is mainly due to the poor constraint of the decay index. Chandra observations are not very long and occurs days after the burst. On the other hand, one need either a fast observation or a very long observation of the afterglow to obtain a good constraint on the decay index. We thus cannot use these observations to set constraints on the burst environment.

We can note that jet features are excluded most of the time. When we cannot exclude them, we also cannot exclude any other model. This does not rule out the possibility of a collimated fireball, but simply put a lower limit to the jet opening angle, which should be larger than $0.166(n_1/E_{52})^{1/8}$ rad (where n_1 is the density in cm^{-3} units and E_{52} the total energy of the burst). This may indicate a possible large beaming angle.

We can finally note that due to a degeneration in two closure relationships, we cannot discriminate the burst environment from a wind profile or a constant ISM medium when the cooling frequency, ν_c, is below the X-ray band. One notable exception is GRB 040106, which should be, according to the closure relationship, surrounded by a wind profile. The authors of ref. [3] have shown that the optical observations agree with this interpretation and that the cooling frequency is above the X-ray band 6 hours after this burst.

3˙2. *Absorption around GRBs.* – We examine the optical *vs.* X-ray fluxes diagram as in [7]. Because we are now comparing fluxes, we need to use a common epoch for all bursts. We have used (as in [7]) the value of 11 hours after the burst (this corresponds to ~ 40 kiloseconds after the burst, an epoch where BeppoSAX observed most of his burst afterglows). This imply for all burst an interpolation or extrapolation of the flux. The uncertainties on the values obtained, the late observation dates, and the uncertainties about possible break into the light curve prevent us to obtain meaningful values for

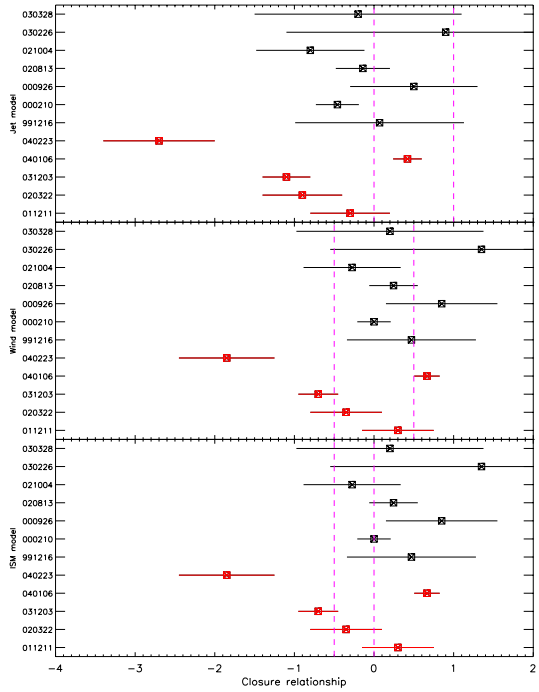

Fig. 1. – The closure relationship for all burst with constraints on both the spectral and temporal decay indexes. Vertical lines indicate the theoretical expected values. Afterglows observed by Chandra are located at the top (in black), while those observed by XMM-Newton are located at the bottom (in red, see electronic version for colors).

Chandra afterglows. We have thus used here only XMM-Newton results.

We present the optical *vs.* X-ray fluxes diagram in fig. 2 (indicating afterglows from BeppoSAX and XMM-Newton). All the values have been corrected for the galactic absorption (X-ray) or extinction (R band), using [12]. Not all XMM-Newton bursts are displayed in this figure: three GRBs in our sample do not have detected optical afterglows. We do not include the corresponding upper limits in fig. 2 due to the poor constrains they put on them. We indicate the best fit relationship obtained from the data, including (dashed line) and excluding (solid line) from the fit the upper limits.

However, GRB 020322 is very interesting because it is located in the "dark" side of the figure: it is a normally bright X-ray afterglow, while it displays a faint optical afterglow. This burst also displays an excess of X-ray absorption [14]. Using a galactic gas-to-dust law the authors of ref. [14] indicated that this burst is optically extincted. Using the more correct dust-to-gas law of [1] indicated in the work of [13], we calculated an extinction of 1.6 ± 0.4 magnitudes in the R band (taking into account all the uncertainties of the spectral fit). Assuming that the ratio of the optical to X-ray afterglow fluxes (taken 11 hours after the burst) is constant, the relationships displayed in fig. 2 imply an extinction of 0.5–2.5 magnitudes for GRB 020322, compatible with our finding from the X-ray. An X-ray absorption similar to the one measured in the case of GRB 040223 would have implied an optical extinction large enough to prevent the detection of any optical afterglow (making this burst dark) : some dark GRB may be due to absorption.

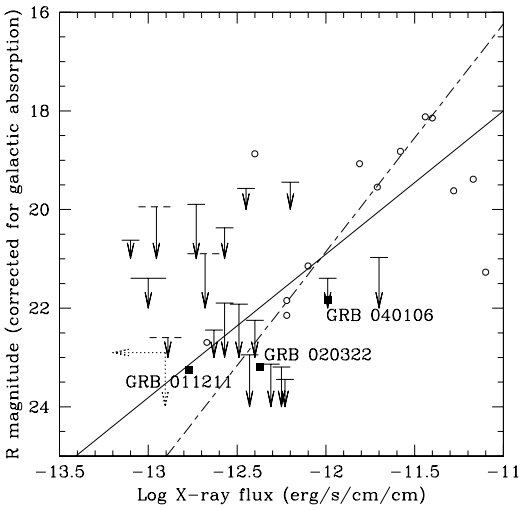

Fig. 2. – Optical *vs.* X-ray fluxes of GRB afterglows 11 hours after the burst. Squares and open circles represent XMM-Newton and Beppo-SAX data extracted from [4] and [7], respectively. Lines indicate the best-fit relationships (see text for details).

3˙3. *X-ray afterglows properties*. – We also found that GRBs are segregated in two groups depending on their flux and decay index: the dim afterglows appears to decay slower than the bright ones. We refer the reader to Gendre and Boër (these proceedings) for details and discussion.

* * *

This work was supported by the EU FP5 RTN "Gamma ray bursts: an enigma and a tool". We acknowledge the use of the web page of J. Greiner (`http://www.mpe.mpg.de/~jcg/grbgen.html`).

REFERENCES

[1] Calzetti D., Kinney A. L. and Storchi-Bergmann T., *ApJ*, **429** (1994) 582.
[2] Chevalier R. A. and Li Z. Y., *ApJ*, **520** (1999) L29.
[3] Gendre B., Piro L. and DePasquale M., *A&A*, **424** (2004) L27.
[4] Gendre B., Corsi A. and Piro L., *A&A* in preparation.
[5] Meszaros P. and Rees M. J., *ApJ*, **476** (1997) 232.
[6] Panaitescu A., Meszaros P., and Rees M. J., *ApJ*, **503** (1998) 314.
[7] De Pasquale M., Piro L., Perna R. *et al.*, *ApJ*, **592** (2003) 1018.
[8] Piro L., in *Third Rome Workshop on GRB in the Afterglow Era*, edited by Feroci M., Frontera F., Masetti N. and Piro L., *ASP Conf. Ser.*, Vol. **312** (2004) 149.
[9] Rees M. J. and Meszaros P., *MNRAS*, **258** (1992) 41.
[10] Rhoads J. E., *ApJ*, **487** (1997) L1.
[11] Sari R., Piran T. and Narayan R., *ApJ*, **497** (1998) L17.
[12] Schlegel D. J., Finkbeiner D. P. and Davis M., *ApJ*, **500** (1998) 525.
[13] Stratta G., Fiore F., Antonelli L. A. *et al.*, *ApJ*, **608** (2004) 846.
[14] Watson D., Reeves J. N., Osborne J. P. *et al.*, *A&A*, **395** (2002) L41.